Formation of stable, two-dimensional alloy-surface phases: Sn on Cu(111), Ni(111), and Pt(111)

S. H. Overbury and Yi-sha Ku
Oak Ridge National Laboratory, Oak Ridge, Tennessee 37831-6201
(Received 2 March 1992)

Results are summarized of ion-scattering analysis of the surface structure obtained following deposition and annealing of ultrathin layers of Sn on Cu(111), Ni(111), and Pt(111). It is found that on each substrate, annealing to about 0.4 of the substrate melting temperature gives rise to a stable structure characterized by a $p(\sqrt{3}\times\sqrt{3})$-$R30°$ low-energy electron diffraction pattern and $\frac{1}{3}$ monolayer coverage. The surfaces are isostructural and correspond to rippled surface alloy which is a single layer thick. The measured rippling, in which Sn atoms protrude outward from neighboring substrate atoms, is found to be linearly related to the substrate lattice constant suggesting that rippling provides lateral strain relief within the layer. Issues of the depth distribution, the thermal stability, the preferential formation of the $p(\sqrt{3}\times\sqrt{3})$-$R30°$ ordering, and the measured rippling are discussed in light of the ion-scattering results and theoretical studies of surface alloys.

The interdiffusion of an ultrathin metal overlayer with a metallic substrate has not been well characterized in very many cases (for a good review see Ref. 1). In most cases the structure, composition, and depth distribution of the interdiffused layers are not known or predictable. Deposition of metals on metals presents an alternative approach to studies of alloy surfaces and a way to produce more readily controllable compositions. Such surfaces may exhibit configurations and properties not obtainable at alloy surfaces.

We present here results which summarize alkali ion scattering and low-energy electron diffraction studies of the interaction of Sn with the (111) surfaces of Ni, Cu, and Pt. We find that when Sn layers [thickness on the order of one monolayer (ML)] evaporated onto the substrates are annealed to within a certain temperature range, the Sn incorporates into the substrate surface rather than forming an overlayer structure. This result is not unexpected in view of the fairly high solubility of Sn in each substrate and the fact that several intermetallic compounds form between Sn and the substrate metals. The more interesting result is that in each case the surface readily forms a two-dimensional alloy phase with Sn coverage of $\frac{1}{3}$ ML, and with a $p(\sqrt{3}\times\sqrt{3})$-$R30°$ ordering that is a single monolayer thick. The surface reaches this state by rapid dissolution of excess Sn (i.e., amounts larger than $\frac{1}{3}$ ML) into the bulk. The resulting ordered monolayer is then quite stable against coverage changes, depth redistribution, or reordering. Strain due to size mismatch is accommodated in the monolayer by surface rippling, the extent of which depends linearly upon the mismatch. These results underscore the necessity to consider the formation of structurally identifiable surface phases in formulating a description of surface segregation at dilute alloy surfaces.

The details of these studies are presented elsewhere.[2,3] Sn is deposited evaporatively upon clean single-crystal substrates in UHV and analyzed by Auger electron spectroscopy (AES), low-energy electron diffraction (LEED), and low-energy alkali-ion scattering. The latter probe is used to analyze the structure of the resulting surface using blocking and shadowing effects. Following deposition the surface is annealed to various temperatures and the resultant changes are characterized.

On all three substrates, Ni(111), Cu(111), and Pt(111), it is found that a structure identified by LEED to have a $p(\sqrt{3}\times\sqrt{3})$-$R30°$ symmetry is formed predominantly upon annealing. This structure is readily formed when the initially deposited Sn coverage is at least $\frac{1}{3}$ ML but may be in excess of 1 ML. Comparison of the angle dependence of the ion scattering from all three surfaces indicated that these surfaces are isostructural and correspond to the incorporated, rippled monolayer structure shown in Fig. 1. The Sn is incorporated into the first substrate layer rather than existing as an overlayer. The evidence for this is derived from ion scattering at a variety of conditions and is as follows: (1) scattering features expected for overlayer Sn shadowing substrate atoms were *not* found at predicted locations, (2) features expected for incorporated Sn shadowing substrate atoms *were* found at their predicted locations, at least for Sn/Ni(111) and

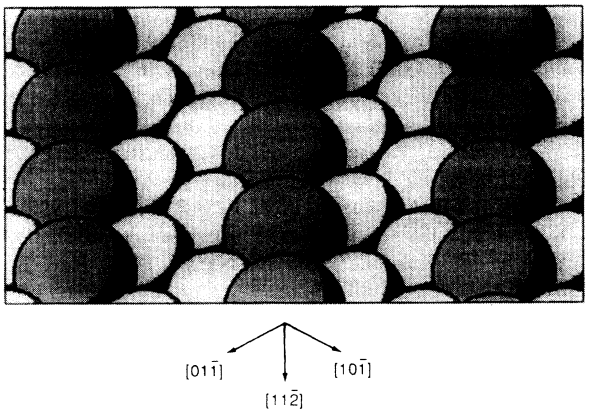

FIG. 1. A ball model shows the rippled $p(\sqrt{3}\times\sqrt{3})$-$R30°$ surface alloy structure. The relative atom radii and extent of rippling are shown for Sn/Ni(111). The structure is viewed at an oblique angle (70° from surface normal) causing foreshortening along the [11$\bar{2}$] direction.

Sn/Cu(111), (3) comparison between the alloy surface $Pt_3Sn(111)$ and Sn/Pt(111) (Ref. 4) showed similarities in the angle dependence indicative of comparable first-layer total atomic densities, (4) scattering from Sn at very grazing angles is too weak and featureless to be explained by scattering from a sparse (i.e., $\frac{1}{3}$ ML) overlayer, but is indicative of shadowing within a denser mixed layer, and (5) locations of Sn single-scattering critical edges were consistent with an incorporated (but rippled) surface.

DEPTH DISTRIBUTION OF ALLOY SURFACE

It is found that the $p(\sqrt{3}\times\sqrt{3})$-$R30°$ structure can be produced in such a way that it is a single monolayer thick. Ion scattering is well suited for demonstrating this fact. Incident angle scans are shown in Fig. 2 which demonstrate the ability to distinguish first-layer from deeper-layers scattering. The upper scan shows a scan of the Cu single scattering from clean Cu(111). A low-angle edge at around 15° marks the onset of scattering from first-layer atoms which is the dominant contribution at the Cu single scattering energy up to about 35°. The sharp, intense "subsurface layer" peak at about 52° corresponds to the critical angle with respect to $[00\bar{1}]$ rows, so near this angle, scattering from second and third layers becomes dominant. The incident angle scan is characteristic of fcc(111) surfaces for this azimuth and scattering angle and similar scans are obtained for Ni(111) and Pt(111). If a second type of atom is present on lattice sites just below the surface, then single scattering from this atom will give rise to a similar subsurface layer peak. This effect has been seen in alloy and in second-layer growth of pseudomorphic overlayers.[5,6]

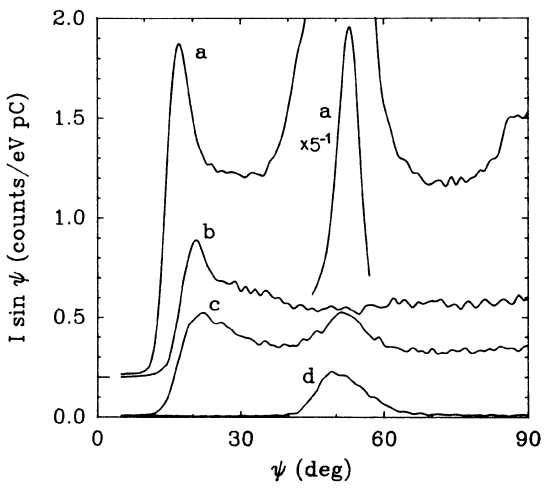

FIG. 2. Incident angle dependence of the Li^+ ion scattering intensity (sine corrected) is shown for scattering in the $[11\bar{2}]$ azimuth for laboratory scattering angle of 130° and incident ion energy $E_i=500$ eV. The polar incident angle ψ is measured from the surface plane. Curves are shown for different relative final energy E/E_i from the various surfaces; (a) $E/E_i=0.697$ (Cu single scattering) from clean Cu(111), (b) $E/E_i=0.811$ (Sn single scattering) from $p(\sqrt{3}\times\sqrt{3})$-$R30°$ Sn/Ni(111), (c) $E/E_i=0.811$ from $p(\sqrt{3}\times\sqrt{3})$-$R30°$ Sn/Cu(111); and (d) $E/E_i=0.811$ from clean Cu(111). Curves (a) and (b) are offset for clarity.

Scans are shown in Figs. 2(b) and 2(c) of the Sn single scattering for the $p(\sqrt{3}\times\sqrt{3})$-$R30°$ structure for Sn/Ni(111) and for Sn/Cu(111) at the same scattering conditions as in scan (a). For Sn/Ni(111) it is seen that the Sn scan exhibits a sharp edge around 18° indicating the onset of scattering from first-layer Sn, but the scan exhibits no trace of a subsurface peak near 52° indicating that there is no Sn present in the second or third layers, within the experimental sensitivity of ≤ 0.01 ML.

A similar scan for Sn/Cu(111), Fig. 2(c), does exhibit a peak near $\psi=52°$, possibly suggesting the presence of subsurface Sn. However, examination of the energy distribution in this region reveals that this feature is due to multiple scattering from the substrate. In this range of angles the scattering from the Cu substrate is very intense and multiple-scattering features appear above the Cu single-scattering energy ($E/E_i=0.697$). The tailing edges of these features overlap the Sn single-scattering energy ($E/E_i=0.811$). It was found that this effect accounts for the apparent subsurface contribution observed for Sn/Cu(111) as demonstrated by scan (d) in Fig. 2. It is concluded that, like Sn/Ni(111), it is possible to prepare the $p(\sqrt{3}\times\sqrt{3})$-$R30°$ structure in the Sn/Cu(111) system so that near-surface Sn is present only in the top layer.

This test of layer thickness could not be conducted for the Sn/Pt(111) case. In this situation the Sn single scattering is at an energy below that for Pt single scattering and is therefore present upon the large substrate multiple-scattering background. This interference prevented accurate observation of the Sn single-scattering intensity at large angles of incidence. However, the similarities in the ion scattering and the Sn Auger data suggest that the $p(\sqrt{3}\times\sqrt{3})$-$R30°$ Sn/Pt(111) structure is analogous to Sn/Cu(111) and Sn/Ni(111) and stabilizes at a single monolayer thickness.

These results therefore show that the $p(\sqrt{3}\times\sqrt{3})$-$R30°$ structures are truly two-dimensional phases. This arrangement is common for chemisorbed nonmetallic overlayers, e.g., S or O overlayers, but is less well established for metallic (or semimetallic) adsorbates which have a large solubility in and large negative enthalpies of mixing with the substrate metal. Perhaps the most important factor in establishing such a sharp depth distribution is the relative difference in surface energy. However, the relative tendency of the adsorbate to form delocalized metallic bonds versus covalent bonds or to accept bulk coordination may be a factor in the case of Sn adsorbate.

STABILITY OF THE $p(\sqrt{3}\times\sqrt{3})$-$R30°$ STRUCTURES

It is of interest to determine the thermal range of stability of the $p(\sqrt{3}\times\sqrt{3})$-$R30°$ structure. In their studies of Sn/Pt(111), Paffett and Windham[7] performed 1-min anneals at sequentially higher temperature on a surface which had nearly 3 ML of Sn deposited upon it at 140 K. They found that when they reached annealing temperatures of about 700 K (about $0.35T_m$, where T_m is the melting temperature of the substrate), the ratio of Sn/Pt

ion-scattering peak intensities stabilized. Although the LEED pattern at this point was not reported, the conditions were such that a $p(\sqrt{3}\times\sqrt{3})$-$R30°$ structure should have been present. In later experiments[2] it was reported that flashing a Sn layer to 975 K ($0.48T_m$) consistently yielded a $p(\sqrt{3}\times\sqrt{3})$-$R30°$ structure for all initial coverages greater than about $\frac{1}{3}$ ML. These observations suggest that excess Sn above the $\frac{1}{3}$ ML required to form the $p(\sqrt{3}\times\sqrt{3})$-$R30°$ structure rapidly (time scale on the order of 1 min) diffuses into the bulk (or into thick Sn islands or droplets) for annealing temperatures above about $0.35T_m$, yet the remaining $\frac{1}{3}$ ML remains in the top layer at temperatures as high as $0.5T_m$. Above this temperature Sn desorbs from the surface. For Sn on the Ni(111) substrate, the $p(\sqrt{3}\times\sqrt{3})$-$R30°$ structure formed from several initial Sn coverages in the range from $\frac{1}{3}$ ML to above 1 ML upon annealing at 1000 K ($0.58T_m$) and all initial coverages gave roughly the same final Sn AES intensity. Annealing experiments indicated that the $p(\sqrt{3}\times\sqrt{3})$-$R30°$ structure formed readily at temperatures of 650 K ($0.38T_m$).[3]

The stability for the $p(\sqrt{3}\times\sqrt{3})$-$R30°$ structure was studied in more detail on the Cu(111) surface. For room-temperature-deposited Sn coverages in the range of 0.4–0.7 ML, it was found that structural changes and Sn diffusion, as indicated by AES and ion scattering, occurred after a short anneal at 500 K ($0.37T_m$), but the transition to the $p(\sqrt{3}\times\sqrt{3})$-$R30°$ structure was not complete. A short (about 1 min) anneal at 600 K ($0.44T_m$) was sufficient to complete the transition to $p(\sqrt{3}\times\sqrt{3})$-$R30°$ structure and reduced the Sn Auger intensity to that characteristic of the $p(\sqrt{3}\times\sqrt{3})$-$R30°$ structure. Subsequent anneals for several minutes at 600 K resulted in no further change in the Sn AES signal, the ion-scattering energy distribution, or the incident-angle dependence shown in Fig. 3(a). It was found that annealing to temperatures of 900 K ($0.66T_m$) would degrade the $p(\sqrt{3}\times\sqrt{3})$-$R30°$ structure to a surface which has slightly lower coverage of 0.20–0.25 ML and numerous defects, as demonstrated by the decreased overall intensity and the growth of the low-angle feature in Figs. 3(b) and 3(c). This low-angle feature is indicative of shadowing of Sn by neighboring Cu atoms, as distinct from shadowing by neighboring Sn which occurs for the perfectly ordered $p(\sqrt{3}\times\sqrt{3})$-$R30°$ structure. The effect is large because of rippling in the surface and a similar effect is also seen for Sn/Pt(111) in comparing the $p(2\times2)$ and $p(\sqrt{3}\times\sqrt{3})$-$R30°$ surfaces.[2] In the case of Sn/Cu(111) the surface still exhibits a weak $p(\sqrt{3}\times\sqrt{3})$-$R30°$ LEED pattern after the 900-K anneals and no sign of $(\frac{1}{2},\frac{1}{2})$ order beams. Extensive annealing at 600 K of a surface slightly depleted in Sn (by annealing at 900 K) did not recover the Sn coverage to $\frac{1}{3}$ ML. This indicates that once the Sn diffuses away from the surface it becomes lost to the bulk. Annealing the $p(\sqrt{3}\times\sqrt{3})$-$R30°$ structure to 1000 K ($0.74T_m$) for about 1 min gave a drop in Sn coverage to around 0.2 ML. The low-angle edge in Fig. 3(d) indicates loss of $p(\sqrt{3}\times\sqrt{3})$-$R30°$ ordering.

The conclusion from the data in all these systems is that annealing to $0.35–0.4T_m$ is sufficient to activate

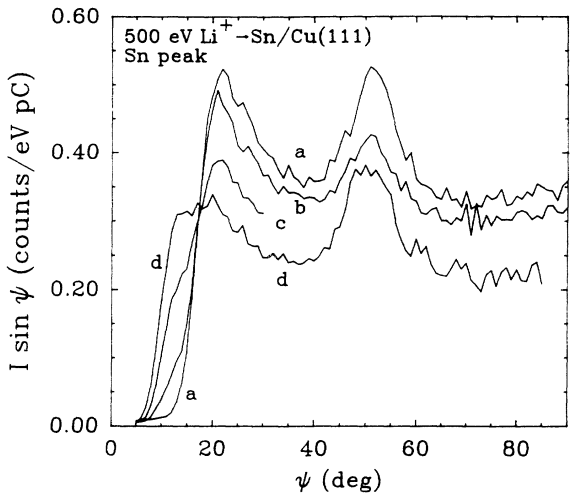

FIG. 3. As in Fig. 2 with $E/E_i=0.811$ (Sn single-scattering energy) for (a) the $p(\sqrt{3}\times\sqrt{3})$-$R30°$ Sn/Cu(111) surface annealed to 600 K, (b) after annealing surface in (a) to 900 K for 2–3 min, (c) after annealing surface in (b) to 900 K for an additional 5 min (partial scan), and (d) after annealing $p(\sqrt{3}\times\sqrt{3})$-$R30°$ surface to 1000 K for about 1 min, leaving a Sn coverage determined by AES to be about 0.2 ML.

structure conversion, place exchange, and diffusion of deposited Sn into the bulk. Above the temperatures of the activated formation, the $p(\sqrt{3}\times\sqrt{3})$-$R30°$ structures are stable or at least metastable to temperatures as high as $0.5–0.6T_m$ as long as this temperature is below about 1000 K, where Sn desorption begins to occur at a significant rate. Although the $p(\sqrt{3}\times\sqrt{3})$-$R30°$ structure is a very stable configuration, it is probably not representative of full equilibrium in these cases, for the reason that the bulk Sn composition is essentially zero. However, it is possible a very dilute bulk Sn composition might be sufficient to completely stabilize this structure.

In the Sn/Cu(111) and the Sn/Ni(111) surface the only ordered structure observed by LEED was the $p(\sqrt{3}\times\sqrt{3})$-$R30°$ structure: in particular, a $p(2\times2)$ structure was not observed. It was not determined whether a Sn deposition very near $\frac{1}{4}$ ML would lead to a $p(2\times2)$ structure on Cu(111) or Ni(111). However, initial deposits in excess of $\frac{1}{3}$ ML, upon annealing always evolved into a $p(\sqrt{3}\times\sqrt{3})$-$R30°$ structure. For the case of Sn/Cu(111), annealing to 900 K to reduce the Sn composition to near or below $\frac{1}{4}$ ML did not yield a $p(2\times2)$ structure but only gave a weakened $p(\sqrt{3}\times\sqrt{3})$-$R30°$ structure. For Sn/Pt(111) a $p(2\times2)$ pattern was observed if the amount of deposited Sn was roughly 0.25 ± 0.03. Initial deposits of greater than about 0.3 ML readily stabilized at the $p(\sqrt{3}\times\sqrt{3})$-$R30°$ structure upon annealing. Deposition of additional Sn on a $p(2\times2)$ surface and annealing would also cause conversion to the $p(\sqrt{3}\times\sqrt{3})$-$R30°$ structure. Therefore, in all three systems, if a sufficient amount of Sn was available, the $p(\sqrt{3}\times\sqrt{3})$-$R30°$ structure appeared to be strongly preferred to a $p(2\times2)$. Recent theoretical work by Teraoka[8] predicts the relative stability of a $p(\sqrt{3}\times\sqrt{3})$-

$R30°$ surface ordering compared to a surface $p(2\times2)$ ordering for dilute fcc alloys A_xB_{1-x} which exhibit $p(2\times2)$ ordering in bulk (111) planes of the intermetallic compound $A_{0.75}B_{0.25}$. For the case in which only the first layer is different from the bulk concentration, the situation encountered in the present experiments, the predicted order-disorder transition temperature for ordering to $p(\sqrt{3}\times\sqrt{3})$-$R30°$ structure is always higher than that to order into a $p(2\times2)$ structure and therefore the latter will not form. Using Monte Carlo calculations and the embedded-atom method, Foiles reached a similar conclusion for the system of Au deposited on Cu(111).[9] Choosing the chemical potentials appropriately to fit a dilute Au content, it was found that a bulk Au concentration of 0.1 at. % was sufficient to stabilize a surface concentration of $\frac{1}{3}$ ML in a $p(\sqrt{3}\times\sqrt{3})$-$R30°$, rippled surface alloy layer. Evidently, in this case also, the $p(\sqrt{3}\times\sqrt{3})$-$R30°$ structure is favored over a $p(2\times2)$ structure. Both of these theoretical results are qualitatively consistent with the present observations.

The $p(\sqrt{3}\times\sqrt{3})$-$R30°$ surface structure is not characteristic of any bulk alloy phase, since intermetallics with the 2:1 stoichiometry of this structure do not form in Cu-Sn, Ni-Sn, or Pt-Sn alloys.[10] Bulk Pt_3Sn and Ni_3Sn exhibit $p(2\times2)$ ordering on their hexagonal (111) and (0001) planes, respectively.[11] Bulk Cu_3Sn with a distorted hcp structure has a modulated $c(4\times2)$ ordering on its quasihexagonal planes.[12] The $p(\sqrt{3}\times\sqrt{3})$-$R30°$ structure therefore seems to be uniquely associated with a surface phase. The preference for $p(\sqrt{3}\times\sqrt{3})$-$R30°$ ordering is affected by the bulk Sn composition. The $p(\sqrt{3}\times\sqrt{3})$-$R30°$ ordering does not occur on $Pt_3Sn(111)$, which instead favors a $p(2\times2)$ ordering identical to the ordering found on bulk (111) planes, and the first layer apparently contains 0.25 ML Sn.[4,13] This provides an interesting situation in which Pt(111) substrate supports a stable, first-layer Sn composition that is higher than for the bulk Pt_3Sn alloy surface.

SURFACE RIPPLING IN THE $p(\sqrt{3}\times\sqrt{3})$-$R30°$ STRUCTURES

Although in each system the Sn is incorporated into the surface and the long-range order and the monolayer distribution appear to be a common feature, there is variation in structural parameters. By ion scattering it was determined that the Sn atoms are not coplanar with their nearest-neighbor first-layer substrate atoms. The Sn buckles outward by an amount $d_\perp$. The extent of this surface rippling was determined directly from the critical angle for Sn single scattering.[2–4] Comparison between all three systems and the Pt_3Sn alloy reinforced the measurement technique and provided checks of key factors such as the Sn scattering potentials. Determination of $d_\perp$ is direct and unaffected by the substrate interlayer relaxation, or by buckling and relaxation in the second or deeper layers.

Measured values of $d_\perp$ are shown in Fig. 4. It is seen that the amount of rippling is linearly correlated to the lattice constant a_0 of the substrate. The Sn atoms have a larger atomic radius than the substrate atoms, so incorporation into the first layer is expected to result in strain within the layer. This strain can be relieved by rippling. This results in the largest value of $d_\perp$ for the smallest lattice size and decreasing rippling as the lattice constant increases. The correlation provides a means of predicting the extent of rippling on other fcc(111) substrates should the incorporated $p(\sqrt{3}\times\sqrt{3})$-$R30°$ Sn structure form on them.

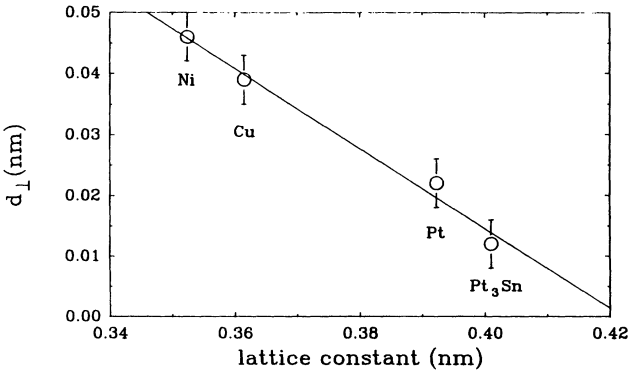

FIG. 4. The measured values of $d_\perp$ are plotted vs the substrate lattice constant for the $p(\sqrt{3}\times\sqrt{3})$-$R30°$ surface of Sn/Ni(111), Sn/Cu(111), and Sn/Pt(111), and for the $p(2\times2)$ surface of the $Pt_3Sn(111)$ alloy.

It is not clear exactly what determines this empirical correlation. These values of $d_\perp$ yield bond distances between first-layer substrate atoms and the Sn atoms, d_1(Sn-X), which are a few percent smaller than the bond distances found in the corresponding SnX_3 alloys, as shown in Table I. The bond distance between Sn and second-layer substrate atoms, d_2(Sn-X), depends upon the first-second interlayer spacing d_{12} of the substrate which has not been measured. Based upon unrelaxed values of d_{12}, the values of d_2(Sn-X) are found to be 4–10 % larger than bulk alloy distances (Table I). In the few cases where there are measurements, it is found that the presence of a larger atom incorporated into the substrate first layer causes a slight outward relaxation of the top-layer substrate atoms (i.e., increase in d_{12}), compared to the clean surface. For example, in $c(2\times2)$ Au/Cu(100) (Ref. 14) and for 0.39 ML of Pt incorporated into Ni(100) (Ref. 15) the top-layer substrate atoms are relaxed outward about 4% and 1%, respectively. Any such outward relaxation in the present system would imply a larger value of d_2(Sn-X). Whether second-layer

TABLE I. Comparison of interatomic distances (in nm).

	$d_\perp$	$a_0/\sqrt{2}$	d_1(Sn-X)	d_2(Sn-X)	$d_{\text{Sn-}X}$(alloy)
Sn/Ni(111)	0.046	0.249	0.253	0.288	0.261–0.264 (Ni_3Sn)
Sn/Cu(111)	0.039	0.256	0.259	0.288	0.271–0.278 (Cu_3Sn)
Sn/Pt(111)	0.022	0.277	0.278	0.296	0.283 (Pt_3Sn)
Pt_3Sn(111)	0.011	0.282	0.283	0.294	0.283 (Pt_3Sn)

buckling occurs is probably not known for any such system, but it appears that the Sn strikes a compromise position between contracted d_1(Sn-X) and expanded d_2(Sn-X) bond distances. A rippling is also found on $Pt_3Sn(111)$ alloy surface. In this alloy bulk Sn and Pt atoms are coplanar in (111) planes with a $p(2\times2)$ ordering. The fact that there is rippling on this surface is a reminder that redistribution of electronic charge at the surface creates relaxation which also plays a role in producing the rippling in bimetallic surfaces, especially if there are ionicity differences in the two components.[16]

These data provide a stringent test for theoretical models which attempt to predict structures at metal or alloy surfaces, the challenge being to predict the stability of the $p(\sqrt{3}\times\sqrt{3})$-$R30°$ ordering in the first layer and to quantitatively predict the amount of the rippling. Experimentally, these surfaces provide well-defined structures which would be excellent candidates for a full LEED study to look for relaxations or rippling in the second and third layers. It would also be of interest to determine how the stability of the $p(\sqrt{3}\times\sqrt{3})$-$R30°$ structure depends upon bulk composition up to the Sn solubility limit. Examination of the (100) and (110) surfaces would provide information about whether incorporation and ordered surface alloy formation occurs on these substrates and, if so, how the magnitude of the surface rippling depends upon first-layer versus second-layer coordination.

ACKNOWLEDGMENTS

This research was sponsored by Division of Chemical Sciences, Office of Basic Energy Sciences, U.S. Department of Energy under Contract No. DE-AC05-840R21400 with the Martin Marietta Energy Systems, Inc.

[1]C. T. Campbell, Annu. Rev. Phys. Chem. **41**, 775 (1990).
[2]S. H. Overbury, D. R. Mullins, M. T. Paffett, and B. C. Koel, Surf. Sci. **254**, 45 (1991).
[3]Yi-sha Ku and S. H. Overbury, Surf. Sci. **273**, 353 (1992).
[4]S. H. Overbury and P. N. Ross (unpublished).
[5]S. H. Overbury and D. R. Mullins, J. Vac. Sci. Technol. A **7**, 1942 (1989).
[6]S. H. Overbury, D. R. Mullins, M. T. Paffett, and B. E. Koel in *The Structure of Surfaces* III, edited by S. Y. Tong, M. A. Van Hove, K. Takayanagi, and X. D. Xie (Springer-Verlag, New York, 1991).
[7]M. T. Paffett and R. Windham, Surf. Sci. **208**, 34 (1989).
[8]Y. Teraoka, Surf. Sci. **235**, 249 (1990).
[9]S. M. Foiles, Surf. Sci. **191**, 329 (1987).
[10]F. A. Shunk, *Constitution of Binary Alloys, Second Supplement* (McGraw-Hill, New York, 1969); M. Hansen, *Constitution of Binary Alloys* (McGraw-Hill, New York, 1958).
[11]P. Villars and L. D. Calvert, *Pearsons Handbook of Crystallographic Data for Intermetallic Phases* (American Society for Metals, Metals Park, OH, 1985).
[12]Y. Watanabe, F. Fujinaga, and H. Iwasaki, Acta Crystallogr. Sec. B **39**, 306 (1983).
[13]A. N. Haner, P. N. Ross, and U. Bardi, Surf. Sci. **249**, 15 (1991).
[14]Z. Q. Wang, Y. S. Li, C. K. C. Lok, F. Jona, and P. M. Marcus, Solid State Commun. **62**, 181 (1987).
[15]S. Deckers, W. F. van der Weg, and F. H. P. M. Habraken, in *The Structure of Surfaces III* (Ref. 6).
[16]J. I. Lee, C. L. Fu, and A. J. Freeman, Phys. Rev. B **36**, 9318 (1987).